Lawrence Berkeley Laboratory
UNIVERSITY OF CALIFORNIA

Materials & Molecular Research Division

CLASSICAL MODEL FOR LASER-INDUCED NON-ADIABATIC COLLISION PROCESSES

Ann E. Orel and William H. Miller

January 1980

DISCLAIMER

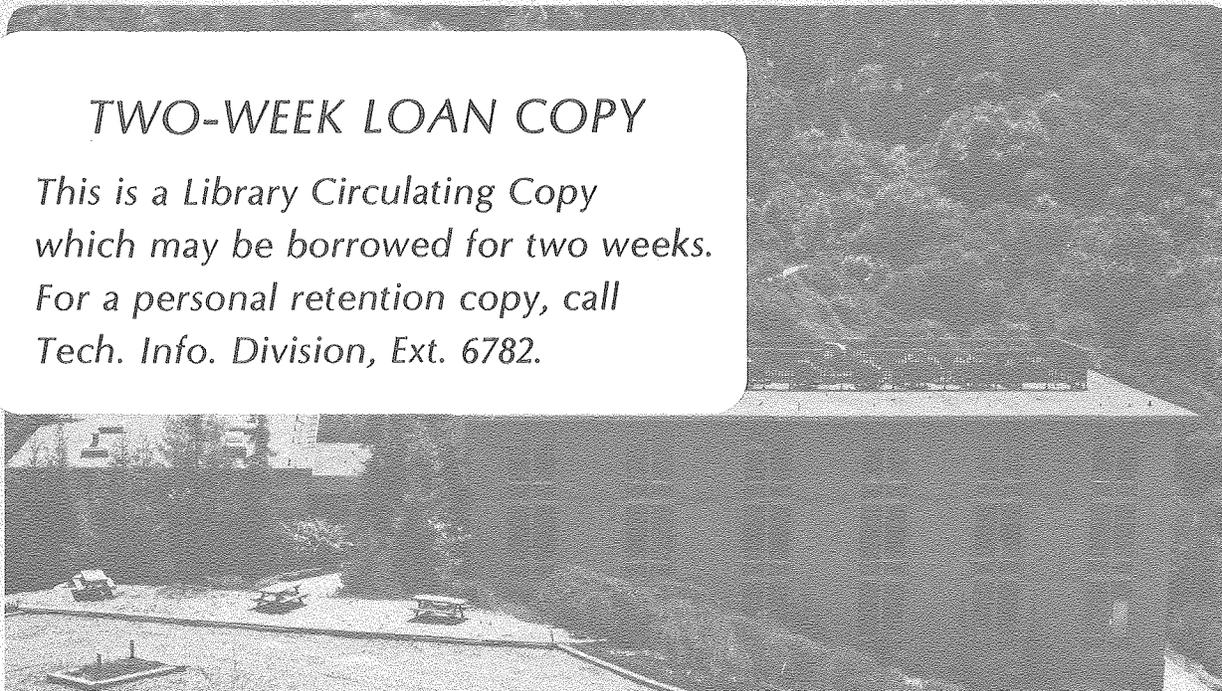CLASSICAL MODEL FOR LASER-INDUCED

NON-ADIABATIC COLLISION PROCESSES

Ann E. Orel and William H. Miller

Department of Chemistry, and Materials and Molecular Research Division
Lawrence Berkeley Laboratory, University of California
Berkeley, California 94720

Abstract

By synthesizing earlier work of Orel and Miller and of Meyer, McCurdy, and Miller, a model for describing laser-induced electronically non-adiabatic collision processes is constructed which treats all degrees of freedom -- heavy particle (i.e., translation, rotation, and vibration), electronic, and photon -- by classical mechanics. This then makes it relatively easy to carry out calculations to simulate such processes within a dynamically consistent framework. Application is made to the test case $H + LiF \rightarrow Li + HF$ reaction considered by Light and Altenberger-Siczek. The most interesting feature revealed by these classical calculations is maxima in the reaction probability as a function of initial translational energy at energies below the laser-free threshold. It is seen that this structure can be understood as a Franck-Condon-like effect.

I. Introduction

There has been considerable interest recently in how high power lasers affect molecular collision processes. Most papers on the topic have been theoretical,[1-5] although there have been some reports[6-10] of experiments which show these effects. Most workers, both theoretical and experimental, have dealt with the effect of visible/UV lasers, i.e., those which can cause electronic excitations, but it has been pointed out[5] that high power infrared lasers can also modify collision processes (e.g., increase rate constants for chemical reactions) without causing electronic excitation.

The purpose of this paper, which also considers the effect of visible/UV lasers on collision phenomena, is two-fold. First, we show how a completely classical model can be constructed for such processes, i.e., one which describes the nuclear motion (translation, rotation, and vibration), electronic degrees of freedom, and the laser radiation field all by classical mechanics and thus in a dynamically consistent framework. The usefulness of this kind of approach is apparent if one wishes to describe molecular collision phenomena, e.g., atom-diatom inelastic and reactive collisions: the large number of quantum states (electronic, vibrational, rotational, and photon) involved makes quantum mechanical treatments extremely difficult and limited to special cases (e.g., collinear A + BC collision systems). With the classical model described below, on the other hand, calculations can be carried out with standard classical trajectory methods; for A + BC collisions, for example, the only difference from the standard situation is that there are two additional classical degrees of freedom, the electronic degree of freedom and the photon degree of freedom. Quantum effects,

if they are thought to be significant, can be incorporated to some extent within the "classical S-matrix" model.[11]

This classical model, which we develop in Section II, is essentially a synthesis of two earlier developments: Orel and Miller[5] have developed (and applied) a classical model for molecular collisions on <u>one</u> potential energy surface (i.e., one adiabatic electronic state) in a radiation field—i.e., a model which treats the nuclear degrees of freedom (i.e., translation, rotation, and vibration) and the photon degree of freedom by classical mechanics—and Meyer, McCurdy, and Miller[12] have developed a model for electronically non-adiabatic collision processes which treats the nuclear degree of freedom and the electronic degrees of freedom all classically. Here, therefore, we present a classical model which treats <u>everything</u> — nuclear degrees of freedom, electronic degrees of freedom, and the photon degrees of freedom—classically. Again, the advantage of this approach is that it is straightforward, via numerical integration of the classical equations of motion, to describe the interaction of all these degrees of freedom dynamically consistently.

The second purpose of the paper is to apply this classical model to a test problem, the reaction

$$LiF + H \rightarrow Li + HF \qquad (1)$$

as considered by Light and Altenberger-Siczek,[4b] who carried out quantum mechanical coupled-channel calculations. The interest is to see how the reaction probability is affected by a visible/UV laser which can cause electronic excitation during the collision. The results of our classical model are consistent with the quantum results, where the latter

exist, but more importantly, we investigate a wider range of initial collision energies and this reveals an interesting structure in the energy dependence of the reaction probability: at energies below the threshold for reaction without the laser, the reaction probability is significantly enhanced at particular collision energies (which depend on the frequency of the laser). This effect is understood as a Franck-Condon-like effect and should pertain in general. This and other aspects of the classical calculations for laser-induced reaction are presented and discussed in Section III.

II. The Classical Model

The classical Hamiltonian for a molecular system and a single mode radiation field has the standard form

$$H = H_{mol} + H_{rad} + H_{int} \quad , \qquad (2.1)$$

where the various terms are the molecular Hamiltonian, which involves nuclear (i.e., translational, rotational, and vibrational) and electronic degrees of freedom, the Hamiltonian for the pure radiation field, and the interaction between the two, respectively. If (x, p) denote the nuclear coordinates and momenta and (n, q) the classical action-angle variables for the electronic degrees of freedom (assuming a 2-state electronic system), then the Meyer-McCurdy-Miller[12] theory gives the molecular Hamiltonian as

$$H_{mol}(p, x, n, q) = \frac{p^2}{2m} + (1-n)H_{00}(x) + nH_{11}(x)$$
$$+ 2\sqrt{n(1-n)} \, H_{01}(x)\cos q \quad , \qquad (2.2)$$

where $H_{n,n'}(x)$, $n, n' = 0, 1$, is the diabatic electronic potential energy surface. If (N, Q) are the classical action-angle variables of the radiation field, then the Orel-Miller theory[5] gives H_{rad} and H_{int} (in the dipole approximation) as

$$H_{rad} = \hbar \omega N \qquad (2.3)$$

$$H_{int} = -\sqrt{\frac{8\pi\hbar\omega}{V}} \, \sqrt{N} \, \cos Q \, \mu(x, n, q) \quad , \qquad (2.4)$$

where ω is the frequency of the laser, V the volume of the radiation cavity, and $\mu(\underset{\sim}{x},n,q)$ is the component of the molecular dipole moment along the polarization vector of the laser. Finally, to express the dipole moment μ as a function of the classical electronic action-angle variables (n,q) we invoke the Heisenberg correspondence relation as discussed by McCurdy and Miller;[12a] this gives

$$\mu(\underset{\sim}{x},n,q) = (1-n)\mu_{00}(\underset{\sim}{x}) + n\mu_{11}(\underset{\sim}{x})$$

$$+ 2\sqrt{n(1-n)}\ \mu_{01}(\underset{\sim}{x})\ \cos q \quad , \qquad (2.5)$$

where $\mu_{n,n'}(\underset{\sim}{x})$, $n,n' = 0,1$ is the matrix of the dipole moment operator in the 2-state electronic basis, as a function of the nuclear coordinates $\underset{\sim}{x}$.

Combining Eqs. (2.1)-(2.5) gives the complete classical Hamiltonian for the nuclear $(\underset{\sim}{p},\underset{\sim}{x})$, electronic (n,q), and photon (N,Q) degrees of freedom as

$$H(\underset{\sim}{p},\underset{\sim}{x},n,q,N,Q) = \frac{\underset{\sim}{p}^2}{2m} + (1-n)H_{00}(\underset{\sim}{x}) + nH_{11}(\underset{\sim}{x})$$

$$+ 2\sqrt{n(1-n)}\ H_{01}(\underset{\sim}{x})\cos q + \hbar\omega N \qquad (2.6)$$

$$- \sqrt{\frac{8\pi\hbar\omega}{V}}\ \sqrt{N}\ \cos Q[(1-n)\mu_{00}(\underset{\sim}{x}) + n\mu_{11}(\underset{\sim}{x}) + 2\sqrt{n(1-n)}\mu_{01}(\underset{\sim}{x})\cos q].$$

From this Hamiltonian one can numerically integrate Hamilton's equations in the standard way.[13] Initial conditions for the nuclear coordinates and momenta $(\underset{\sim}{x},\underset{\sim}{p})$ are specified in the usual way,[13] and for the electronic and photon variables, the initial values of n and N are integers, the

initial electronic state and the initial number of photons in the radiation field, respectively. If the popular quasiclassical model[13] is employed, then q and Q are chosen initially by Monte Carlo sampling methods. (Section IIIA discusses this in more detail).

For the application in the next section, the Hamiltonian of Eq. (2.6) is simplified following Light et al:[4b]

$$H_{01} = \mu_{00}(\underset{\sim}{x}) = \mu_{11}(\underset{\sim}{x}) = 0 \qquad . \qquad (2.7)$$

Setting $H_{01} = 0$ corresponds to neglecting electronically non-adiabatic effects in the absence of the radiation field, and setting $\mu_{00}(\underset{\sim}{x}) = \mu_{11}(\underset{\sim}{x}) = 0$ corresponds to neglecting the interaction of nuclear motion within a given electronic state with the radiation field (the Orel-Miller process[5b,c]); at the frequency of laser employed here (i.e., visual/UV), this latter interaction is indeed negligible. The quantities $H_{00}(\underset{\sim}{x})$ and $H_{11}(\underset{\sim}{x})$ are thus the two adiabatic electronic potential energy surfaces $V_0(\underset{\sim}{x})$ and $V_1(\underset{\sim}{x})$, respectively, so that the Hamiltonian of Eq. (2.6) simplifies to

$$H(\underset{\sim}{p},\underset{\sim}{x},n,q,N,Q) = \frac{p^2}{2m} + (1-n)V_0(\underset{\sim}{x}) + n\,V_1(\underset{\sim}{x}) + \hbar\omega N$$
$$- \sqrt{\frac{8\pi\hbar\omega}{V}}\; 2\sqrt{Nn(1-n)}\;\; \mu_{01}(\underset{\sim}{x})\,\cos Q\,\cos q. \qquad (2.8)$$

This is the classical Hamiltonian used for the applications in the next section. (The usual Langer-like modification[12] -- i.e., in the last term, $\sqrt{n(1-n)} \rightarrow \sqrt{(n+\frac{1}{2})(\frac{3}{2}-n)}$ -- is also made to Eq. (2.8). N is so large that replacing N by $N + \frac{1}{2}$ has no significant effect).

III. Application of LiF + H → Li + HF

A. Methodology

Light et al[4b] considered a collinear version of the above reaction, and this is the example we also treat, using the same two potential energy surfaces as these authors used. (The parameters defining the two LEPS potential surfaces are given in Table II of Ref. 4b). The classical Hamiltonian of Fig. (2.8) then defines the collision system, and the calculations reported below (Section IIIC) were carried out within the standard quasi-classical model.

The methodology of quasi-classical trajectory calculations is well-known.[13] For this example, there are two nuclear degrees of freedom, i.e., $(\underset{\sim}{p},\underset{\sim}{x}) \equiv (P,p,R,r)$, where (R,P) are the coordinate and momentum for relative translation of LiF and H, and (r,p) are the coordinate and momentum for vibration for LiF. $(\tilde{n},\tilde{q})$ denote the vibrational action-angle variables for LiF, and $r(\tilde{n},\tilde{q})$ and $p(\tilde{n},\tilde{q})$ are the algebraic functions which express the cartesian vibrational variables in terms of their action-angle variables.

The initial conditions (at time t_1) for a trajectory are then specified as

$$\left.\begin{array}{l} n(t_1) = n_1 \text{ (the electronic quantum number)} = 0 \text{ or } 1 \\[4pt] N(t_1) = N_1 \text{ (the photon quantum number)} = \text{integer} \\[4pt] q(t_1) = q_1 \\[4pt] Q(t_1) = Q_1 \\[4pt] r(t_1) = r(\tilde{n}_1, \tilde{q}_1) \\[4pt] p(t_1) = p(\tilde{n}_1, \tilde{q}_1) \end{array}\right\} \quad (3.1)$$

where $\tilde{n}_1$ is an integer, the initial vibrational state,

$$R(t_1) = \text{large}$$

$$P(t_1) = -\sqrt{2\mu E_{tr}}$$

If χ_r $(q_1, Q_1, \tilde{q}_1, n_1, N_1, \tilde{n}_1; E_{tr})$ is the <u>characteristic function for reaction</u>--i.e., $\chi_r = 1$ if the trajectory with the indicated initial conditions is reactive, and is 0 otherwise--then the total reaction probability for initial quantum numbers n_1, N_1, $\tilde{n}_1$ and initial translational energy E_{tr} is

$$P_r(n_1, N_1, \tilde{n}_1; E_{tr}) = (2\pi)^{-3} \int_0^{2\pi} dq_1 \int_0^{2\pi} dQ_1 \int_0^{2\pi} d\tilde{q}_1 \ \chi_r(q_1, Q_1, \tilde{q}_1, n_1, N_1, \tilde{n}_1; E_{tr}). \quad (3.2)$$

The integrals over q_1, Q_1, and $\tilde{q}_1$ are performed by Monte Carlo.

The explicit form of Hamilton's equations for the present example are (since Light <u>el al</u>[4b] assume that $\mu_{01}(\underset{\sim}{x}) = \mu_{01}$ is coordinate independent)

$$\left.
\begin{aligned}
\overset{\circ}{r} &= \frac{\partial H}{\partial p} = p/m \\[2ex]
\overset{\circ}{R} &= \frac{\partial H}{\partial P} = P/\mu \\[2ex]
\overset{\circ}{q} &= \frac{\partial H}{\partial n} = V_1(r,R) - V_0(r,R) - \mu_{01}\sqrt{\frac{8\pi\hbar\omega}{V}} \frac{\sqrt{N} \ (1-2n)}{\sqrt{(n+\frac{1}{2})(\frac{3}{2}-n)}} \quad \cos Q \cos q \\[2ex]
\overset{\circ}{Q} &= \frac{\partial H}{\partial N} = \hbar\omega - \mu_{01}\sqrt{\frac{8\pi\hbar\omega}{V}} \frac{\sqrt{(n+\frac{1}{2})(\frac{3}{2}-n)}}{\sqrt{N}} \quad \cos Q \cos q \\[2ex]
\overset{\circ}{p} &= -\frac{\partial H}{\partial r} = -(1-n) \frac{\partial V_0}{\partial r} - n \frac{\partial V_1}{\partial r}
\end{aligned}
\right\} \quad (3.3)$$

$$\overset{\circ}{P} = -\frac{\partial H}{\partial R} = -(1-n)\frac{\partial V_0}{\partial R} - n\frac{\partial V_1}{\partial R}$$

$$\overset{\circ}{n} = -\frac{\partial H}{\partial q} = -\mu_{01}\sqrt{\frac{8\pi\hbar\omega}{V}}\ 2\sqrt{N(n+\tfrac{1}{2})(\tfrac{3}{2}-n)}\ \cos Q\ \sin q \quad ,$$

$$\overset{\circ}{N} = -\frac{\partial H}{\partial Q} = -\mu_{01}\sqrt{\frac{8\pi\hbar\omega}{V}}\ 2\sqrt{N(n+\tfrac{1}{2})(\tfrac{3}{2}-n)}\ \sin Q\ \cos q \quad ,$$

which are integrated with our usual variable step-size predictor-cor-rector algorithm.[11]

B. Qualitative Discussion

Before presenting the results of these trajectory calculations, it is useful to discuss some qualitative aspects of the process. Figure 1 shows a sketch of the energy profiles —the potential energy along a "reaction coordinate" — for the two potential energy surfaces. Referring to this figure, one sees that the ground state potential energy surface has an activation barrier of ~ 0.4 eV, so with no laser present the reaction probability as a function of initial translational energy should have a threshold of ~ 0.4 eV. With a laser of frequency ω, though, the electronic energy gap $V_1 - V_0$ comes into resonance with the laser when classical motion on the (initial) ground state surface reaches the position s_0 indicated in Fig. 1, i.e., s_0 is the value for which $V_1 - V_0 = \hbar\omega$. For initial translational energies $E_{tr} \geq V_0(s_0)$, therefore, classical motion will reach this position and there will be the possibility of resonant electronic excitation; if this happens, then reaction (to electronically excited Li* + HF) occurs with high probability because motion on the excited potential surface is "down-hill all the way" to products.

Qualitatively, therefore, one expects a laser of frequency ω to reduce the threshold of the reaction to approximately $V_0(s_0)$. (Note that for the surfaces in Fig. 1, $V_0(s_0)$ _decreases_ _with_ _increasing_ _ω_). It is also clear that an initial translational energy $E_{tr} \simeq V_0(s_0)$ is the _optimum_ translational energy for reaction (below the laser-free threshold of ~ 0.4 eV) because in this case the classical motion _spends_ _the_ _most_ _time_ in the resonant region $V_1 - V_0 \simeq \hbar\omega$, i.e., for higher translational energies, the classical motion will pass the "resonance region" with finite velocity and thus have a smaller probability of being electronically excited.

The primary qualitative effect of the laser is thus to _cause_ _a_ _peak_ _in_ _the_ _reaction_ _probability_ at the translational energy $E_{tr} \simeq V_0(s_0)$, i.e., where the classical turning point on the ground state potential surface coincides with the resonance region $V_1(s_0) - V_0(s_0) = \hbar\omega$. This is the classical version of a Franck-Condon effect, and one can characterize this behavior semi-quantitatively by calculating the electronic transition probability in the Landau-Zener approximation to the curve-crossing picture in the electronic-field representation.[1,2] (One considers the two potential curves V_1 and $V_0 + \hbar\omega$). Within this model, the probability of the electronic transition $0 \to 1$ with photon transition $N \to N - 1$ is given by

$$P_{1,N-1 \leftarrow 0,N} = 1 - e^{-\delta} \tag{3.4}$$

with

$$\delta = \frac{2\pi}{\hbar v} \frac{\mu_{01}^2 \overline{E^2}}{|\Delta V_0'|}$$

where
$$\overline{E^2} = \frac{2\pi\hbar\omega N}{V}$$

$$\Delta V_0' = V_1'(s_0) - V_0'(s_0)$$

$$v = \sqrt{\frac{2}{m}[E_{tr} - V_0(s_0)]}$$

In this approximation the probability of electronic excitation is 0 for $E_{tr} < V_0(s_0)$, jumps to 1 for $E_{tr} = V_0(s_0)$, and then falls for higher E_{tr}.

For still higher translational energies, $E_{tr} \gtrsim 0.4$ eV, the reaction probability will again rise since reaction can then take place on the ground state potential energy surface. Figure 2 shows a sketch of this expected energy dependence of the reaction probability. One can estimate the <u>width</u> of the Franck-Condon peak in the reaction probability near $E_{tr} \simeq V_0(s_0)$ by determining the value of $E_{tr} - V_0(s_0)$ for which $P = \frac{1}{2}$. Using Eq.(3.4), this "half-width" is easily found to be

$$[E_{tr} - V_0(s_0)]_{P = \frac{1}{2}} = \frac{m}{2}\left[\frac{\mu_{01}^2 \overline{E^2}}{|\Delta V_0'|} \frac{2\pi}{\hbar\ln 2}\right]^2 \quad , \quad (3.5)$$

which is seen to be proportional to the square of the laser intensity.

This qualitative discussion above, which is based on the one dimensional picture of the reaction in Fig. 1, is modified in several ways when the vibrational degree of freedom is taken into account. Most significantly, the Franck-Condon maximum in the cross section below the laser-free threshold will, in general, be <u>split into two</u> <u>maxima</u>. This is because the "Franck-Condon region", i.e., the place where the classical motion spends the most time, is now where the

vibrational motion, as well as the translational motion, experiences a classical turning point. Vibrational motion has two classical turning points, however, so there will be two points on the ground state potential surface where the translational and vibrational motion simultaneously experience classical turning points (i.e., have zero momenta). The electronic energy gap V_1-V_0 will, in general, be different at these two points, and this leads to two different Franck-Condon maxima. (If there were no translation-vibration coupling in the potential energy surfaces and if the vibrational potential functions for the two electronic states were the same, then V_1-V_0 would be the same at the two simultaneous translation-vibration turning points and the two Franck-Condon maxima would be coincident). This will be seen more explicitly in the next section.

C. Results of Trajectory Calculations

Figure 3 shows the total reaction probability as a function of initial translational energy for the quasi-classical trajectory model as described in Section IIIA. LiF is always in its ground vibrational state initially. The dotted curve is the laser-free result, showing the expected threshold at ~ 0.4 eV. The solid curve is obtained for a laser with frequency $\hbar\omega = 6.2$ eV and a power such that $\mu_{01}E_0 = 0.01$ eV ($E_0 = \sqrt{8\pi\hbar\omega N_1/V}$), and the dashed curve is the result for a laser of the same frequency but lower power, $\mu_{01}E_0 = 0.008$ eV.

Both laser-induced curves in Fig. 3 show the two Franck-Condon maxima as discussed at the end of the previous section, and the height and width of the peaks increase with increasing laser power. At the still lower power corresponding to $\mu_{01}E_0 = 0.001$ eV, the peaks have disappeared.

The Franck-Condon peaks in Fig. 3 show the asymmetric "line shape" suggested by the Landau-Zener model discussed in Section IIIB: with increasing translational energy, the reaction probability rises almost vertically to a maximum and then falls more gradually. Quantum mechanical effects may, of course, modify this structure in some of its details, but the gross features are expected to persist in a quantum description.

Figure 4 illustrates the effect of varying the laser frequency. (The laser-free reaction probability is also shown again here). For a power corresponding to $\mu_{01}E_0 = 0.01$ eV, the solid curve is for a frequency $\hbar\omega = 6.2$ eV (the same curve as shown in Fig. 3), and the dashed curve is for a frequency $\hbar\omega = 6.4$ eV. The higher frequency is thus seen to lead to a lower threshold for reaction, as is understood from the discussion in Section IIIB. A surprise though, is that the higher frequency (dashed curve in Fig. 4) has only one peak, not two, in the region below the laser-free threshold.

To understand this latter feature and to confirm that our interpretation of these "Franck-Condon maxima" is actually correct, we computed laser-free classical trajectories on the ground state potential energy surface to determine the Franck-Condon transition points. For a given translational energy E_{tr} (and with LiF initially in its ground vibrational state) the initial vibrational angle variable was varied over its range $(0,2\pi)$ to determine the two points, (r_1,R_1) and (r_2,R_2), at which translation and vibration have simultaneous classical turning points. The electronic energy gaps, V_1-V_0, at these two points define two frequencies, via $\hbar\omega = V_1-V_0$, for which E_{tr} is a Franck-Condon maximum.

Figure 5 shows, as a function of translational energy E_{tr}, these two frequencies $\hbar\omega = V_1(R_k, r_k) - V_0(R_k, r_k)$, where (R_k, r_k), $k = 1,2$ are the two simultaneous turning points for energy E_{tr}. A horizontal line at a given frequency then gives the two translational energies at which Franck-Condon maxima should appear for that laser frequency.

For frequency $\hbar\omega = 6.2$ eV, Fig. 5 thus indicates that Franck-Condon maxima should appear at $E_{tr} \simeq 0.15$ eV and 0.19 eV, and from the Landau-Zener discussion in Section IIIB it is clear that these are actually the energies at which the reaction probability has its sharp verticle rise at these energies.

For the higher frequency, $\hbar\omega = 6.4$ eV, Fig. 5 indicates the two Franck-Condon energies to be $E_{tr} \simeq 0.116$ eV and 0.15 eV. The reaction probability for this frequency (dashed curve in Fig. 4) does indeed show a sharp rise at $E_{tr} \simeq 0.116$ eV and also a broadened structure at $E_{tr} \simeq 0.15$ eV, but it is clear that this is a case for which the two Franck-Condon maxima have merged into a single broadened peak.

It seems clear, therefore, that this Franck-Condon picture of the structure in the reaction probability is physically correct.

Comparing the results of our classical model to the quantum mechanical calculations of Light and Altenberger-Siczek[4b] shows qualitative agreement in that there is essentially no reaction below the classical threshold for the field strength $\mu_{01}E_0 = 0.001$ eV, but substantial reaction at the higher field $\mu_{01}E_0 = 0.01$ eV. There is also agreement in that essentially all the product Li is electronically excited. The agreement for the higher field strength is not quantitative, however, the quantum values being a factor of 2 or so smaller than the classical

results of Fig. 4 in the energy range $E_{tr} \simeq 0.35 - 0.45$ eV. This was

the only energy region reported in the quantum study and unfortunately

is not the region which contains the Franck-Condon structure seen in

the present classical calculations.

IV. Concluding Remarks

One of the purposes of this paper has been to show how a completely classical model can be defined which describes laser-induced non-adiabatic processes. Because calculations can be carried out within the standard quasi-classical framework, it is relatively easy to apply this model to molecular collision processes. It would be quite reasonable, for example, to treat three-dimensional versions of atom-diatom collision systems.

The test case which has been treated is the collinear $H + LiF \rightarrow HF + Li$ reaction considered by Light et al.[4b] To the extent that the present classical calculations can be compared to these quantum calculations, the two are consistent; i.e., at the higher powers, $\mu_{01}E_0 = 0.01$ eV, they both show that the threshold for reaction is lowered by the laser. Unfortunately, however, the quantum calculations were not extended to the energy region where the present classical results show the interesting Franck-Condon structure in the reaction probability.

This Franck-Condon structure in the cross section is certainly the most interesting feature revealed by the present calculations. The fact that a laser of frequency ω will significantly enhance the reaction probability at a particular collision energy E_{tr} (more precisely, in a narrow range of collision energies) is an important point to be aware of: knowing how this Franck-Condon energy varies with ω provides fairly direct information about the potential energy surfaces that are involved in the process, and in a molecular beam experiment, for example, the laser-induced effect will be largest when the collision energy is "tuned" to this Franck-Condon region.

Acknowledgments

References

1. N.M. Kroll and K. M. Watson, Phys. Rev. A13, 1018 (1976).

2a. M. Yuan, T. F. George and F. J. McLafferty, Chem. Phys. Lett. 40, 163 (1976);

 b. J. M. Yuan and T. F. George, J. Chem. Phys. 70, 990 (1979) and other earlier work cited therein.

3a. A. M. F. Lau, Phys. Rev. A13, 139 (1976);

 b. ibid. 19, 1117 (1979), and other earlier work cited therein.

4a. J. C. Light and A. Szöke, Phys. Rev. A18, 1363 (1978);

 b. J. C. Light and A. Altenberger-Siczek, J. Chem Phys. 70, 4108 (1979).

5a. W. H. Miller, J. Chem. Phys. 69, 2188 (1978)

 b. A. E. Orel and W. H. Miller, Chem. Phys. Lett. 57, 362 (1978); J. Chem. Phys. 70, 4393 (1979); ibid. 72, 0000 (1980).

6. W. R. Green, J. Lukasik, J. R. Willison, M. D. Wright, J. F. Young and S. E. Harris, Phys. Rev. Lett. 42, 970 (1979) and earlier work cited therein.

7. V. S. Dubov, L. I. Gudzenko, L. V. Gurvich and S. I. Iakovlenko, Chem. Phys. Lett. 53, 170 (1978), and earlier work cited therein.

8. A. v. Hellfeld, J. Caddick and J. Weiner, Phys. Rev. Lett. 40, 1369 (1978).

9. Ph. Cahuzac and P. E. Toschek, Phys. Rev. Lett. 40, 1087 (1978).

10. P. R. Brooks, private communication.

11. W. H. Miller, Adv. Chem. Phys. 25, 69 (1974).

12a.   W. H. Miller and C. W. McCurdy, J. Chem. Phys. 69, 5163 (1978);

  b.   C. W. McCurdy, H. D. Meyer and W. H. Miller, ibid. 70, 3177 (1979);

  c.   H. D. Meyer and W. H. Miller, ibid. 70, 3214 (1979);

  d.   H. D. Meyer and W. H. Miller, ibid. 71, 2156 (1979).

13.   See, for example, R. N. Porter and L. M. Raff, in Dynamics

       of Molecular Collisions, Part B, Vol. 2 of Modern Theoretical

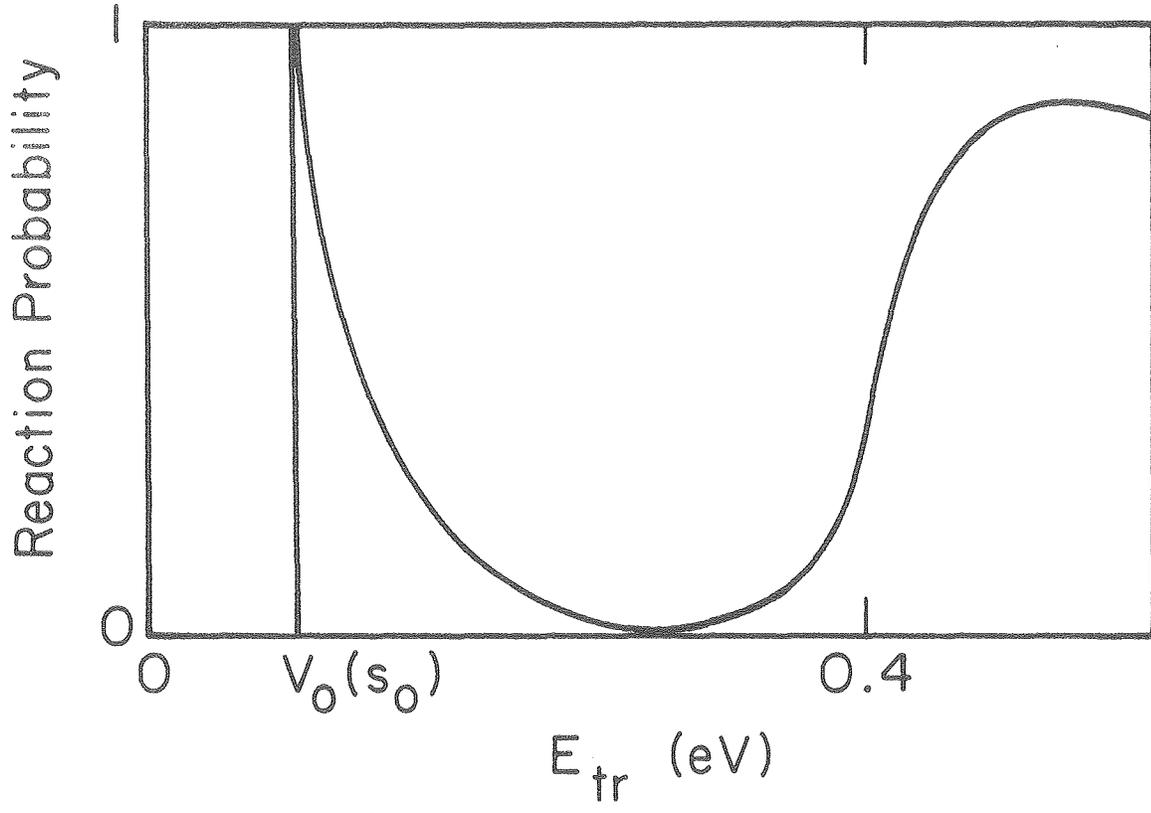   Chemistry, ed. W. H. Miller, Plenum, New York, 1976, pp. 1-50.

Figure Captions

1. Sketch of the potential energy along the reaction coordinate s for
    the two electronic potential energy surfaces for the system
    $H + LiF \rightarrow HF + Li$. E_{tr} denotes the initial translational energy
    and ω the frequency of the laser.

2. Sketch of the qualitative dependence of the total reaction proba-
    bility on initial translational energy E_{tr}.

3. Total reaction probability for $H + LiF \rightarrow HF + Li$ as a function of
    the initial translational energy E_{tr}, from a quasi-classical tra-
    jectory calculation. LiF is initially in its ground vibrational
    state. The dotted curve is the laser-free result. The other
    two curves are for a laser frequency $\hbar\omega = 6.2$ eV, the laser power
    being such that $\mu_{01}E_0 = 0.01$ eV (solid curve) and 0.008 eV (dashed
    curve).

4. Total reaction probability as in Fig. 3. The dotted curve is the
    laser-free result as in Fig. 3. The other two curves are for a
    laser power such that $\mu_{01}E_0 = 0.01$ eV and a frequency $\hbar\omega = 6.2$ eV
    (solid curve) and $\hbar\omega = 6.4$ eV (dashed curve).

5. Shown are the two Franck-Condon frequencies $\hbar\omega \equiv V_1(R_k, r_k) -$
    $V_0(R_k, r_k)$, where (R_k, r_k), $k = 1,2$, are the two simultaneous
    translation-vibration turning points on the ground state poten-
    tial surface, as a function of the initial translational energy
    E_{tr}. The intersection of the dashed line at frequency $\hbar\omega = 6.4$ eV
    with the two curves gives the two translation energies at which
    Franck-Condon maxima should appear for that laser frequency,
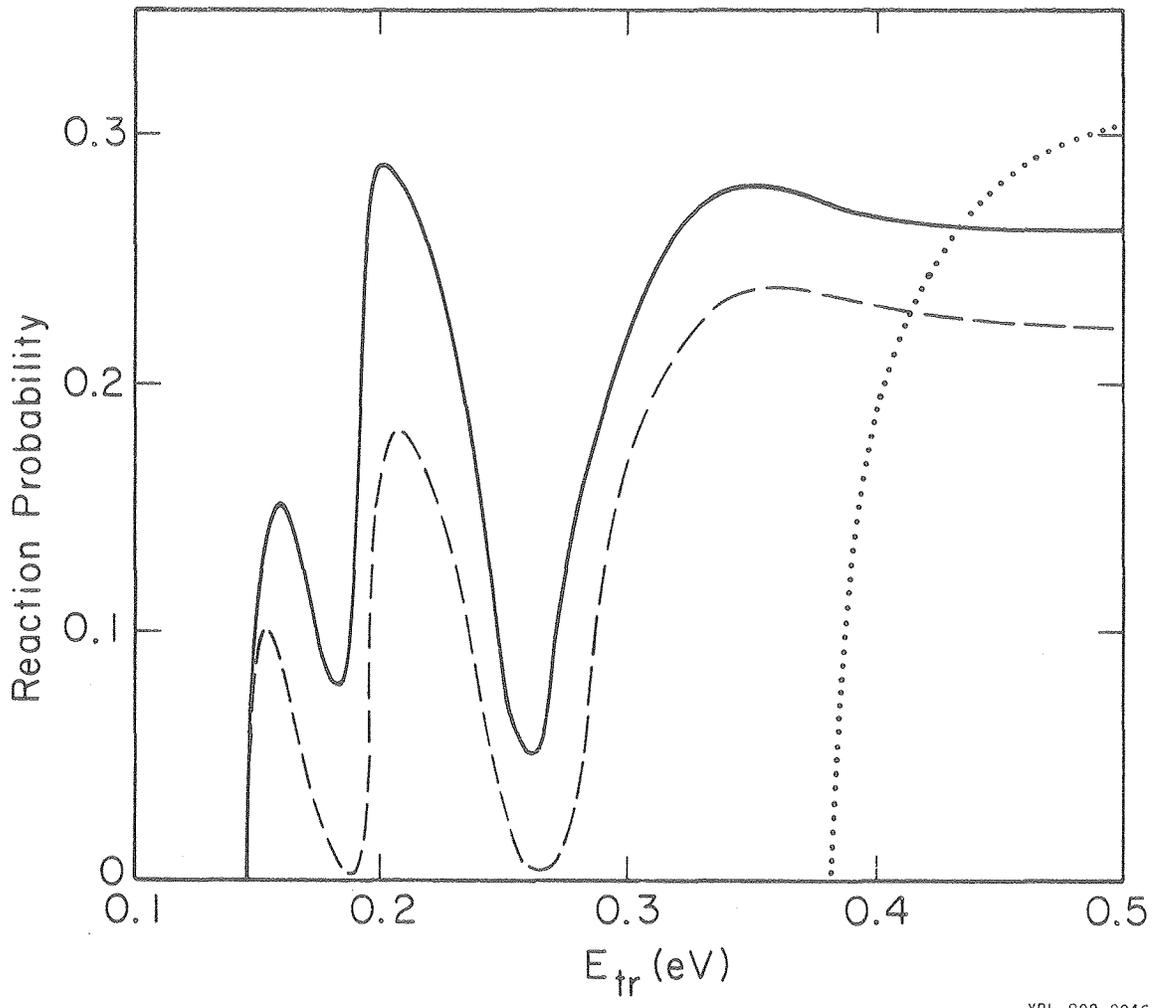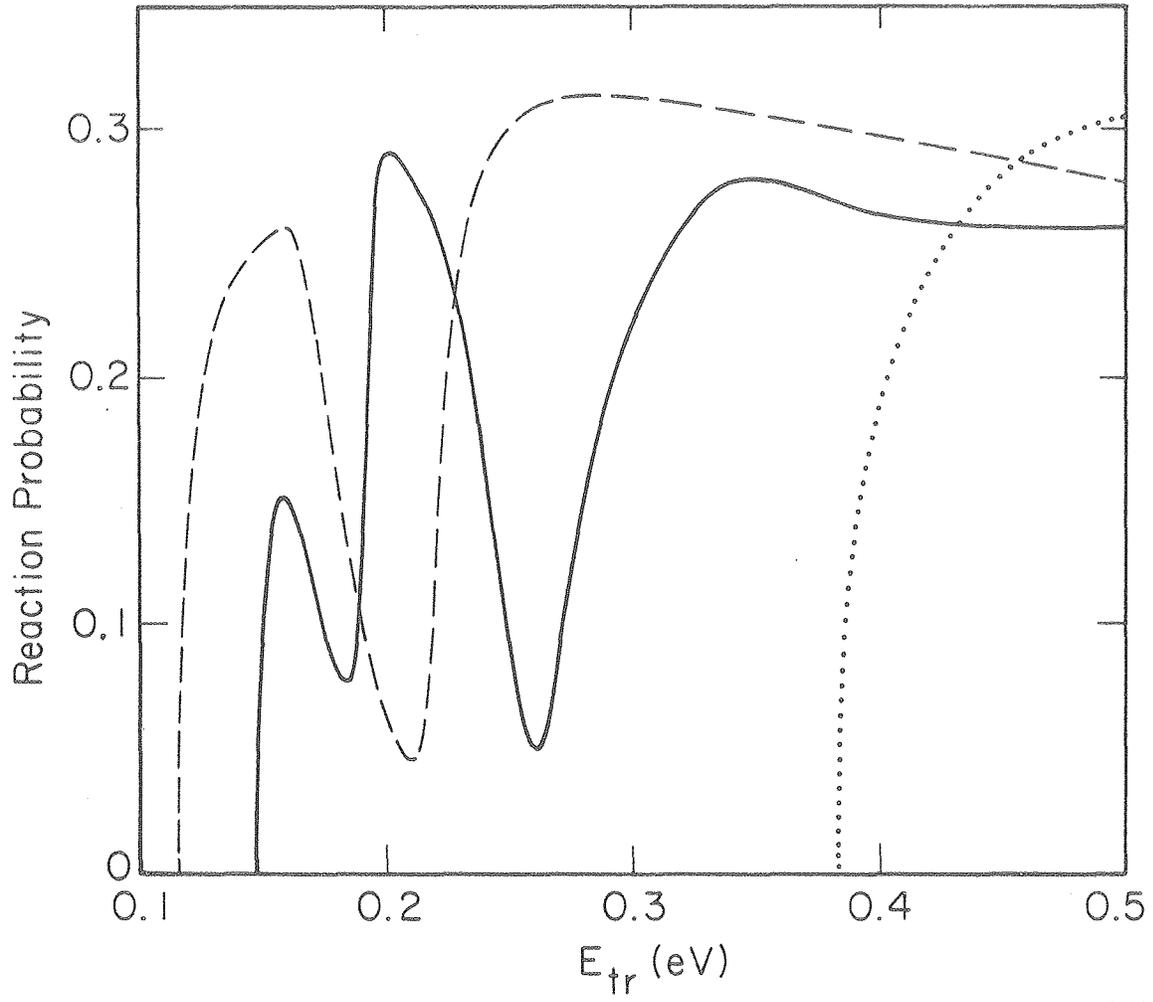   and similarly for frequency $\hbar\omega = 6.2$ eV.
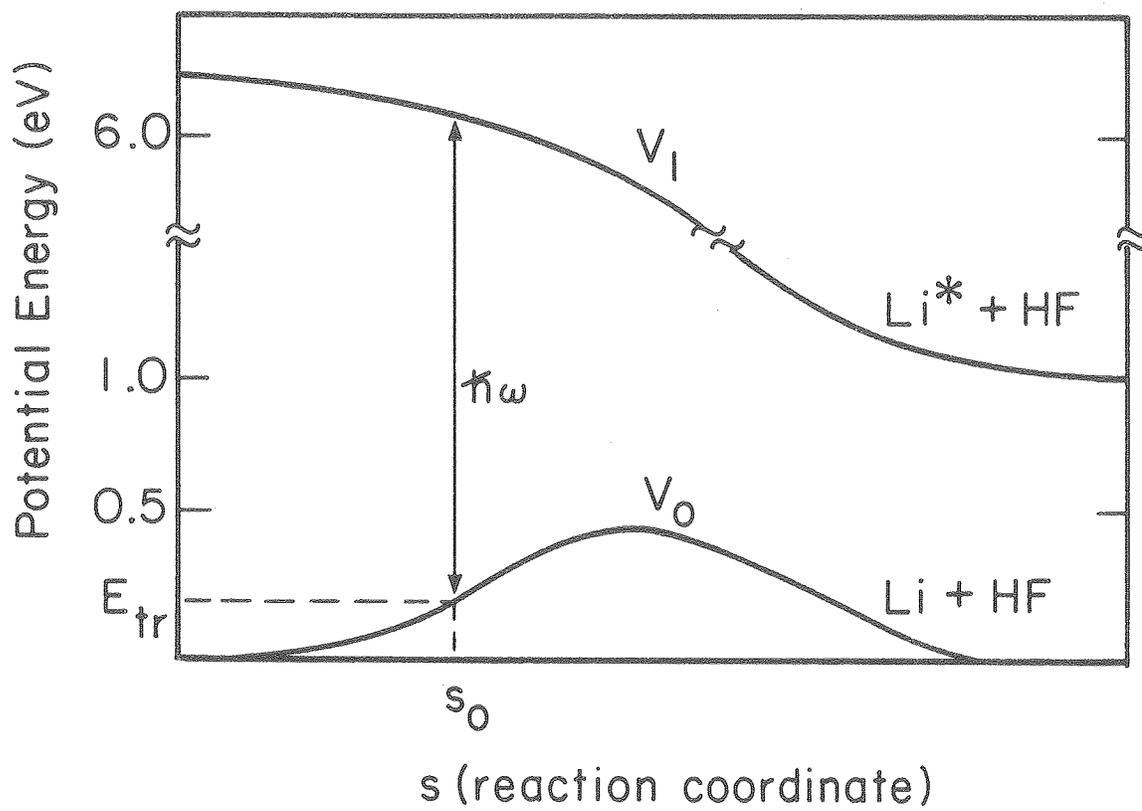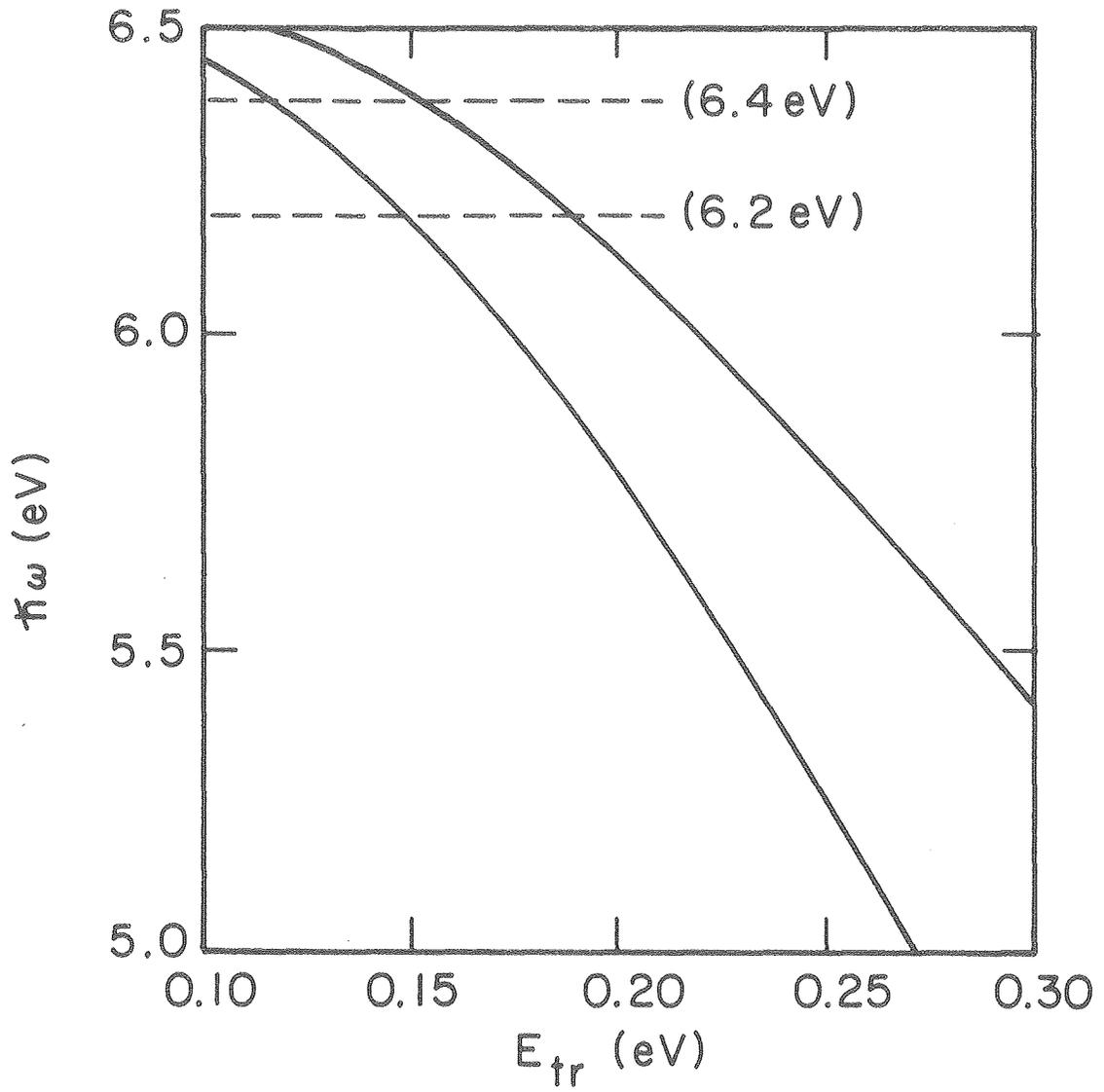
Figure 1

XBL 802-8043

Figure 2

XBL 802-8044

XBL 802-8046

Figure 3

Figure 4

XBL 802-8045

XBL 802-8130

Figure 5